Proceedings of the 2009 IEEE International Conference on Systems, Man, and Cybernetics
San Antonio, TX, USA - October 2009

Permanent Magnet Linear Synchronous Motor Drive Design Based on Sliding-Mode Control and Fuzzy Deadzone Estimation

Ming-Shyan Wang, Ying-Shieh Kung,
Department of Electrical Engineering, Southern Taiwan University
Tainan, Taiwan, R.O.C.
mswang@mail.stut.edu.tw

Cheng-Yi Chiang, and Yi-Ci Wang
kung@mail.stut.edu.tw
m9720209@webmail.stut.edu.tw
bryant.wang@etatung.com.tw

***Abstract*—A permanent magnet linear synchronous motor (PMLSM) digital signal processor-based drive including both sliding-mode controller and fuzzy deadzone estimator is developed to steer the mover position of the PMLSM. The sliding-mode controller with integral operation will provide properties of fast response and insensitive to parameter variations and external disturbance. By utilizing the concept of deadzone compensation to eliminate steady-state errors, the fuzzy deadzone estimator will overcome the problem resulting from the unknown upper bound of lumped uncertainty in sliding-mode control. Finally, the effectiveness of the proposed control schemes is demonstrated by experimental results of tracking square-wave and sinusoidal reference trajectories.**

***Keywords*—permanent magnet linear synchronous motor, sliding-mode controller, fuzzy deadzone estimator**

I. INTRODUCTION

As compared with the rotating permanent magnet synchronous motors (PMSMs), the permanent magnet linear synchronous motors (PMLSMs) are generally applied to the direct-drive mechanical systems to meet the ever increasing demands for higher contouring accuracy at high machine speeds. Many advantages are provided by PMLSM over its indirect counterpart, such as no backlash and less friction, high speed and high precision in long distance locations, a simple mechanical construction resulting in higher reliability and frame stiffness, and a high thrust force [1-6]. However, without using the conventional gears or ball screws, the PMLSM is easier to be affected by load disturbance, torque ripple, and parameter variations. Consequently, the design of a controller with force disturbance compensation is very important in PMLSM drives.

A variable structure system not only is insensitive to parameter variations and external disturbance once it enters the sliding mode, but also has the property of a fast dynamic response. Therefore variable-structure control approaches have been employed in the position and speed control of linear servo systems [4, 7-13]. However, these applications with variable-structure control are subject to difficulty to determine specific and reliable system uncertainty boundaries. As a result, the assumed magnitude of uncertainty boundaries is less than those in real applications such that the existence condition of the sliding mode is violated and control performance deteriorates severely. Using high gain control to improve disturbance rejection is the traditional solution. However, it produces unnecessary deviations from the switching surface and causes large chattering in the control system. The latter causes harmful effects such as current harmonics and acoustic noise in motor drive applications. Serious chattering can be reduced by using the boundary layer where the sign function is replaced by the saturation function. However, it generates the steady state errors. The former may neither maintain the sliding mode nor keep the desired performance. Thus, the system performance will be deteriorated and the steady-state error will occur.

Some of the previous studies investigated algorithms to overcome the bounds of the system uncertainty. In order to improve degraded responses due to uncertainties, a variable-structure controller using a robust fuzzy neural network (RFNN) is investigated, in which the RFNN is utilized to estimate the real-time lumped uncertainty for the position control system [4]. Tian and Guo [10] employed both a sliding-mode tracking controller to ensure the system have fast tracking characteristics to the command and a H_∞ controller to suppress the disturbances within the closed loop. Chen, Liu, and Ting [11] considered a robust integral sliding-mode controller for contouring control of biaxial systems to reduce the effects of the uncertainties. For a stage system levitated and driven by electric magnetic actuators, Jeon et al. [12] designed its sliding-mode position controller to reduce effects from movements and disturbances of other axis. The employment of neural networks with sliding mode control was investigated in the control of a linear drive with flexible transmission element [13].

On the other way, the performance of precise position control systems is typically limited by the non-analytic nature of the actuator nonlinearities, such as deadzone, friction, and backlash. Deadzone is a static nonlinearity that describes the insensitivity of the system to small signals. It represents a “loss of information” when the signal falls into the dead band and can cause limit cycles, tracking errors, steady-state error, etc [14]. Compared with a conventional estimator, a fuzzy inference mechanism uses prior expert knowledge to

978-1-4244-2794-9/09/$25.00 ©2009 IEEE

accomplish the control object more efficiently. The fuzzy inference mechanism can construct the estimation model of the deadzone nonlinearity. Therefore, if we regard the steady-state error as the effect caused by deadzone, we may utilize the fuzzy deadzone estimator [15-17] after the sliding-mode controller to overcome the steady-state error resulted from system uncertainty. As a result, the problem on determining the bound of system uncertainties will be eliminated.

This paper is organized as follows. Section II presents the PMLSM model. Using this model, the control strategy is described in section III. Sections IV and V give the experimental results and conclusions, respectively.

II. MODELING PMLSM

For a PMLSM in the synchronous rotating reference frame, its mathematical model can be described as follows [1-6],

$$\begin{bmatrix} v_q \\ v_d \end{bmatrix} = \begin{bmatrix} R_s + pL_q & \frac{\pi}{\tau} L_d v_e \\ -\frac{\pi}{\tau} L_q v_e & R_s + pL_d \end{bmatrix} \begin{bmatrix} i_q \\ i_d \end{bmatrix} + \begin{bmatrix} \sqrt{2/3}\,\frac{\pi}{\tau}\lambda_{\max} v_e \\ 0 \end{bmatrix} \quad (1)$$

where v_d, i_d, and L_d (v_q, i_q, and L_q) respectively denote the *d*-axis (*q*-axis) voltage, current, and inductance; R_s is the phase-winding resistance; v_e is the electric linear velocity of the mover; $\lambda_{\max}$ is the permanent-magnet flux linkage; τ is the pole pitch; and p denotes the differential operator. Moreover, the linear velocity is $v = v_e / P$, where P is the number of primary pole pairs. The developed electromagnetic force is

$$F_e = P\pi[\sqrt{2/3}\lambda_{\max} i_q + (L_d - L_q) i_d i_q]/\tau \quad (2)$$

and the mover dynamic equation is

$$F_e = M_{mo} pv + D_{mo} v + F_L \quad (3)$$

where M_{mo} is the mass of the moving element system; D_{mo} is the viscous friction and iron-loss coefficient; the subscript index " o " stands for nominal value; and F_L is the external force. With the implementation of field-oriented control and if $i_d = 0$, the PMLSM servo drive can be simplified as:

$$F_e = K_F i_q, \quad K_F = \sqrt{2/3} P\pi\lambda_{\max}/\tau \quad (4)$$

where K_F is the thrust coefficient.

III. CONTROL STRATEGY

Considering a sliding-mode position control of a PMLSM drive shown in Fig. 1, the position error and velocity of the mover are defined as the state variables,

$$x_1(t) = d^* - d, \quad x_2(t) = pd = v; \quad (5)$$

where d and d^* denote the measured position and position command. The system can be represented in the following compact state-space form:

$$p\begin{bmatrix} x_1(t) \\ x_2(t) \end{bmatrix} = \begin{bmatrix} 0 & -1 \\ 0 & -D_{mo}/M_{mo} \end{bmatrix} \begin{bmatrix} x_1(t) \\ x_2(t) \end{bmatrix} + \begin{bmatrix} 0 \\ K_F/M_{mo} \end{bmatrix} i_q(t) + \begin{bmatrix} 0 \\ -1/M_{mo} \end{bmatrix} F_L + \begin{bmatrix} 1 \\ 0 \end{bmatrix} pd^* \quad (6)$$
$$= \mathbf{A}_o \mathbf{x}(t) + \mathbf{B}_o u(t) + \mathbf{D}_o F_L + \mathbf{G} pd^*$$

If the frictional force and the uncertainties introduced by system parameters M_{mo} and D_{mo} are considered,

$$M_m = M_{mo} + \Delta M_m, \quad D_m = D_{mo} + \Delta D_m \quad (7)$$

where " Δ " symbol indicates uncertainty, the system will be modified as

$$p\mathbf{x} = \begin{bmatrix} 0 & -1 \\ 0 & -D_m/M_m \end{bmatrix} \mathbf{x} + \begin{bmatrix} 0 \\ K_F/M_m \end{bmatrix} i_q(t) + \begin{bmatrix} 0 \\ -1/M_m \end{bmatrix} F_L + \begin{bmatrix} 1 \\ 0 \end{bmatrix} pd^* \quad (8)$$
$$= \mathbf{A}_o \mathbf{x}(t) + \mathbf{B}_o (u(t) + E(t))$$

where $E(t)$ is so-called the lumped uncertainty [4, 9].

In order to have zero steady-state error, an integral switching surface is generally designed in the sliding-mode position controller [4, 9],

$$S(t) = \mathbf{C}\mathbf{x}(t) - \mathbf{C}\int_0^t (\mathbf{A}_o + \mathbf{B}_o\mathbf{K})\mathbf{x}(\tau)d\tau \quad (9)$$

where $\mathbf{K}$ is a state-feedback gain matrix and $\mathbf{C}$ is chosen to satisfy $\mathbf{C}\mathbf{B}_o > 0$. Now a position control is proposed as [4, 9],

$$u(t) = \mathbf{K}\mathbf{x}(t) - f_f \cdot sign(S(t)) \quad (10)$$

where $sign(\cdot)$ is the sign function and f_f is chosen to overcome the uncertainties and the sliding condition $S(t)\dot{S}(t) \le 0$,

$$S(t)\dot{S}(t) = S(t)[\mathbf{C}\dot{\mathbf{x}} - \mathbf{C}(\mathbf{A}_o + \mathbf{B}_o\mathbf{K})\mathbf{x}] = S(t)\mathbf{C}\mathbf{B}_o(E(t) - f_f sign(S(t))). \quad (11)$$

That is, the condition of $|E(t)| \le f_f$ satisfies the sliding condition.

If the state trajectory of system (8) hits the switching surface, $S(t) = \dot{S}(t) = 0$, then the equivalent dynamics of system (8) is governed by the following equation:

$$p\mathbf{x} = (\mathbf{A}_o + \mathbf{B}_o\mathbf{K})\mathbf{x} \quad (12)$$

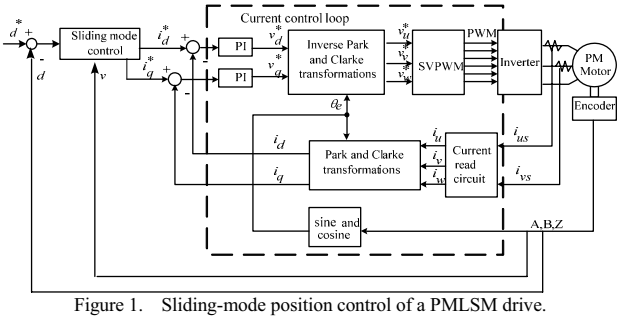

Figure 1. Sliding-mode position control of a PMLSM drive.

It is obvious that the position error $x_1(t)$ will converge to zero exponentially if the poles of system (12) are purposely located on the left-half plane. Thus, the system dynamics will behave as a state-feedback control system. Considering chattering reduction, the following saturation function with linear width of 2ε will replace the sign function in (10),

$$sat(S(t)) = \begin{cases} 1, & S > \varepsilon \\ \dfrac{S}{|S| + \delta}, & |S| < \varepsilon \\ -1, & S < -\varepsilon \end{cases} . \tag{13}$$

However, there exist difficulties on sliding-mode control design on determination of the upper bound the uncertainties f_f in (11). The bound of the uncertainties is so difficult to obtain in advance for practical applications that tracking error will exist in the controlled system. Therefore, based on the position error, a simple but efficient fuzzy deadzone estimator that is described in the aforementioned and shown in Fig. 2 will be proposed here.

The fuzzy control system is a knowledge-based system constructed from a collection of IF-THEN rules. The fuzzy control consists of FI (fuzzification interface), DML (decision making logic), KLB (knowledge base), and DFI (defuzzification interface), shown in Fig. 3 where G_e and G_o are scaling factors. There are nine linguistic variables, PVB (positive very big), PB (positive big), PM (positive medium), PS (positive small), ZE (zero), NS (negative small), NM (negative medium), NB (negative big), and NVB (negative very big) used in the paper. The triangle-shape membership function for fuzzy input and output is shown in Fig. 4. Nine fuzzy control rules are in following form:

$$\text{IF } e \text{ is } f(x) \text{ THEN } CI \text{ is } f(x) \tag{14}$$

where $f(x)$, e, and CI stand for linguistic variable, position error, and fuzzy output, respectively. The expression of defuzzification adopts middle of center method and is given as follows,

$$f_{\_u} = \sum_{m=1}^{N} c_m \mu_m \cdot \left(\sum_{m=1}^{N} \mu_m \right)^{-1} \tag{15}$$

where μ_m, c_m, and $f_{\_u}$ represent the output of membership function, adjusting parameter, and the output of defuzzification, respectively.

Deadzone is a static nonlinearity that describes the insensitivity of the system to small signals. It represents a "loss of information" when the signal falls into the dead band and can cause limit cycles, tracking errors, etc. The nonlinear relation between input $\hat{u}$ and output $T(\hat{u})$ of a non-symmetric deadzone, shown in Fig. 5, is given by

$$T(\hat{u}) = \hat{u} - sat_d(\hat{u}) = \begin{cases} \hat{u} - d_{\_}, & \hat{u} < d_{\_} \\ 0, & d_{\_} \le \hat{u} < d_{+} \\ \hat{u} - d_{+}, & \hat{u} \ge d_{+} \end{cases} \tag{16}$$

$$sat_d(\hat{u}) = \begin{cases} d_{\_}, & \hat{u} < d_{\_} \\ 0, & d_{\_} \le \hat{u} < d_{+} \\ d_{+}, & \hat{u} \ge d_{+} \end{cases} \tag{17}$$

Thus the input and output of the deadzone in the control system are the sliding-mode control and the q-axis current command, and the dead band is adjusted by fuzzy output f_u.

IV. Experimental Results

Fig. 1 shows the block diagram of the sliding-mode controlled position system of the PMLSM, where its parameters are listed in Table 1. The phase currents sensed by hall-effect transducers close the current loop, and the measured speed and position data from an attached linear encoder with a resolution of 5 μm are fed back. DSP TMS320F2407 realizes the blocks of PI (proportional-integral) control, Park, Clarke, inverse Park, and inverse Clarke transformations, ADC, sine and cosine, and SVPWM (space vector pulse-width modulation). The PI control is used to obtain zero steady-state error of d-axis current for completing decoupling condition.

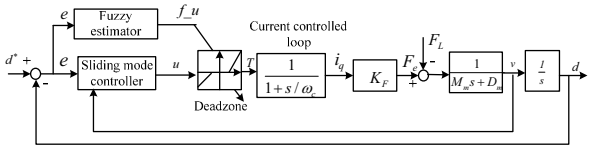

Figure 2. Sliding-mode position control of a PMLSM drive with fuzzy deadzone estimator.

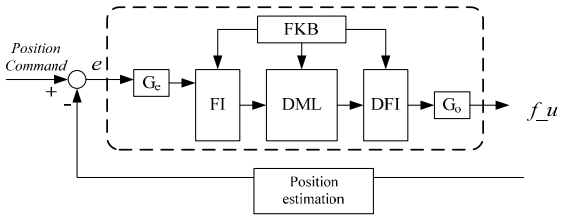

Figure 3. Block diagram of fuzzy control.

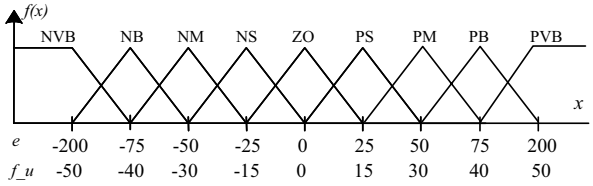

Figure 4. Triangular membership function.

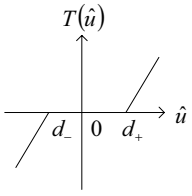

Figure 5. Deadzone nonlinearity.

The design objective is to control the mover to move periodically according to referencing trajectories when the system suffers from parameter uncertainties and disturbance. Firstly, state feedback matrix **K** is simply chosen to be [16 -2] such that the sliding mode equivalent system (12) has eigenvalues of about -8 and -92. Secondly, the constant matrix **C** is chosen to be [50 50] to satisfy $\mathbf{CB}_o > 0$. In addition, the saturation function in (13) has layer width of 100 and the parameter $\delta = 10$. Thirdly, the uncertainty bound is considered to be $f_f = 100$. Respective iron disks weighing 0, 1.5 and 3.5 kg as loading are used to evaluate the performance of the designed sliding-mode controlled system. The 10-to-15 cm square and sinusoidal wave commands with 1 second duration are used to test responsiveness and the tracking ability of the designed control system. The experimental results are depicted in Figs. 6-9. For the square-wave command (blue line), Figs. 6-8 demonstrate related responses (green lines) with respective loading of 0, 1.5 and 3.5 kg. The greater loading, the greater the steady-state error happens at position of 10 cm. In addition, for a 1 Hz sinusoidal command at the condition of no load, Fig. 9 presents the experimental results of (a) mover position (dashed line) and (b) mover position error.

In order to eliminate the effect of bound value of the lumped uncertainty, a simple fuzzy deadzone estimator is added in the sliding-mode system, shown in Fig. 2 where the designed current controlled loop in Fig. 1 is simplified as a first-order low-pass filter with the bandwidth of ω_c [18]. Based on the results in Figs. 6-9, the nominal parameter values of the deadzone in Fig. 5 are set to be $d_- = -50$ and $d_+ = 100$, and the fuzzy output f_u is shown in Fig. 4. Figs. 10-12 demonstrate related square-wave responses (green lines) with respective loading of 0, 1.5 and 3.5 kg. The control effort of the case of 3.5-kg loading is depicted in Fig. 13. It is obvious that the degraded responses are improved while compared with those in Figs. 6-8.

For tracking ability test, Figs. 14(a), 15(a) and 15(b) present 1Hz sinusoidal responses (dashed lines) under the corresponding loads of 0 kg, 1.5 kg, and 3.5 kg. In addition, Figs. 14(b)-(c) show the error, control effort, and uncertainty at no loading, respectively. Even greater chattering occurs in Fig. 14(c) due to large uncertainty upper bound, the system controlled by the proposed algorithm still shows very small tracking error in Fig. 14(b).

V. CONCLUSIONS

We have proposed a DSP-based PMLSM drive that can cope with the position control of respective square-wave and sinusoidal commands. The sliding-mode control has been first designed to deal with parameter variations and external disturbance. Then a very simple but efficient algorithm, fuzzy deadzone estimation, has been employed to deal with the inappropriate selection of the lumped uncertainty bound that yields steady-state errors shown in the experimental results. As a result, the controlled system has demonstrated the effectiveness of the proposed control schemes.

ACKNOWLEDGMENT

The authors would like to express their appreciation to National Science Council for its support under contract NSC 95-2622-E-218-005-CC3.

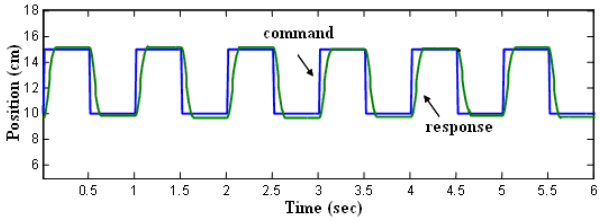

Figure 6. Experimental results for the sliding-mode control system for a square-wave command at the condition of no load.

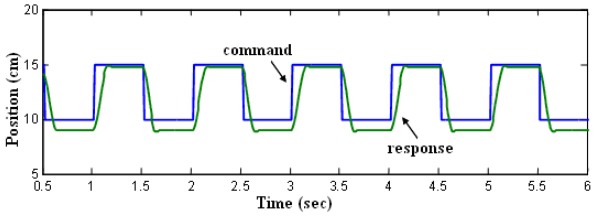

Figure 7. Experimental results for the sliding-mode control system for a square-wave command at the condition of 1.5-kg load.

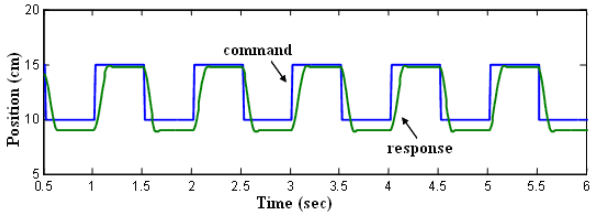

Figure 8. Experimental results for the sliding-mode control system for a square-wave command at the condition of 3.5-kg load.

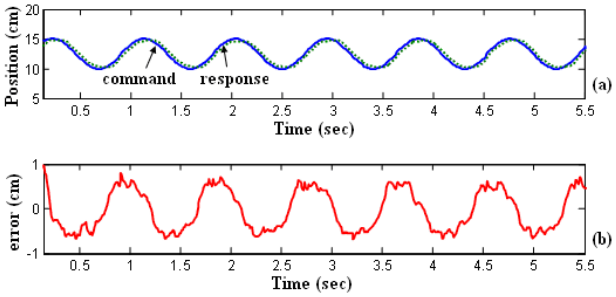

Figure 9. Experimental results for the sliding-mode control system for a sinusoidal command (solid line) at the condition of no load.
(a) Mover position, (b) Mover position error.

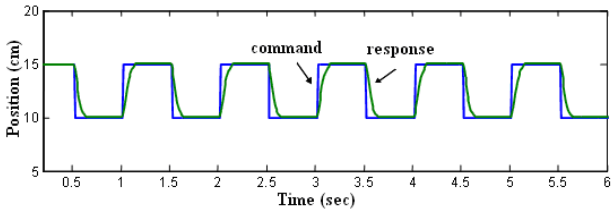

Figure 10. Experimental results for the sliding-mode control system with fuzzy deazone estimation for a square-wave command at the condition of no load.

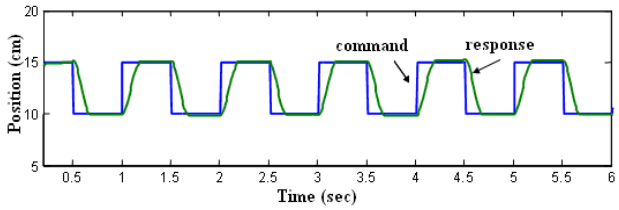

Figure 11. Experimental results for the sliding-mode control system with fuzzy deazone estimation for a square-wave command at the condition of 1.5-kg load.

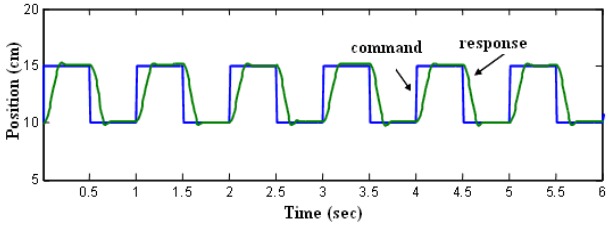

Figure 12. Experimental results for the sliding-mode control system with fuzzy deazone estimation for a square-wave command at the condition of 3.5-kg load.

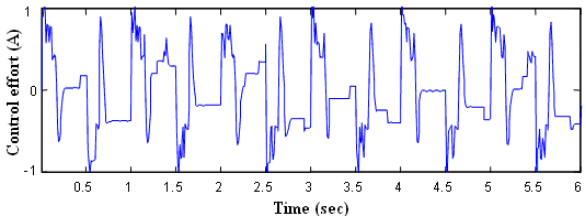

Figure 13. Control effort of the sliding-mode control system with fuzzy deazone estimation for a square-wave command at the condition of 3.5-kg load.

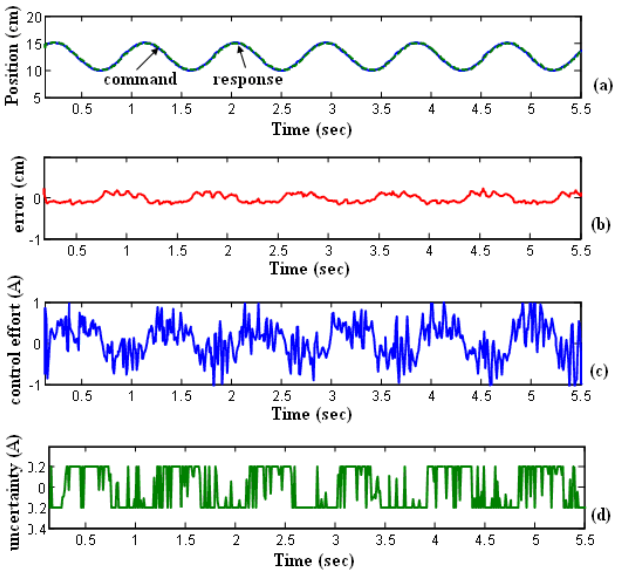

Figure 14. Experimental results for the sliding-mode control system with fuzzy deadzone compensation for a sinusoidal command (solid line) at the condition of no load. (a) Mover position response (dashed line), (b) Mover position error, (c) Control effort, (d) Associated uncertainty.

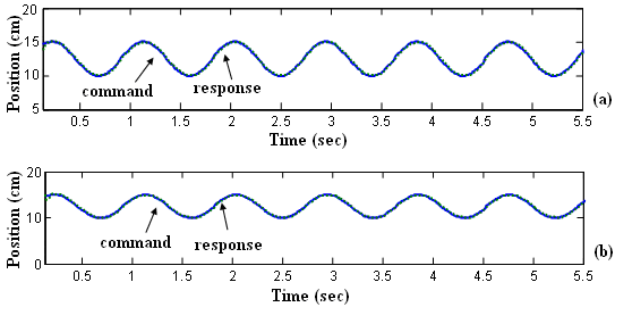

Figure 15. Experimental responses (dashed lines) for the sliding-mode control system with fuzzy deadzone compensation for a sinusoidal command (solid line).
(a) Mover position at the condition of 1.5-kg load,
(b) Mover position at the condition of 3.5-kg load.

TABLE I. PARAMETERS OF PMLSM

Continuous force	F_c	76 N	Length of mover	l_f	206 mm
Rated current	I_c	4 A(rms)	Length of stator	l_s	384 mm
Max. force	F_p	182.4 N	Pole pitch	τ	16 mm
Force constant	K_F	19 N/A	Back emf constant	K_v	18 V/(m/sec)
Mover mass	M_{mo}	0.42 kg	Winding resistance	R_s	4.5Ω
Friction coeff.	D_{mo}	4.12 kg/s	Winding inductance	L_s	0.9 mH

REFERENCES

[1] B.-G. Gu and K. Nam, "A vector control scheme for a PM linear synchronous motor in extended region," IEEE Trans. Industry Applications, vol. 39, no. 5, pp. 1280-1286, 2003.

[2] C. M. Liaw, Y. M. Lin, and K. H. Chao, "A VSS speed controller with model reference response for induction motor drive," IEEE Trans. Industrial Electronics, vol. 48, no. 6, pp. 1136-1147, 2001.

[3] T.-H. Liu, K.-L. Wang, and C.-G. Chen, "Frequency-domain optimal controller design for a permanent magnet linear synchronous motor control system," in Proc. IEEE International Electric Machines and Drives Conf., Madison, Wisconsin USA, 1-4 June, pp. 1525-1531, 2003.

[4] F.-J. Lin, C.-H. Lin, and P.-H. Shen, "Variable-structure control for a linear synchronous motor using a recurrent fuzzy neural network," IEE Proc. Control Theory Applications, vol. 151, no. 4, pp. 395-406, 2004.

[5] C. Rohrig, "Current waveform optimization for force ripple compensation of linear synchronous motors," in 42nd IEEE Conf. on Decision and Control, Hawaii, USA, 9-12 Dec., pp. 5891-5896, 2003.

[6] M. Sanada, S. Morimoto, and Y. Takeda, "Interior permanent magnet linear synchronous motor for high-performance drives," IEEE Trans. Industrial Electronics, vol. 33, no. 4, pp. 966-972, 1997.

[7] C.-T. Pan and T.-Y. Chang, "A fixed structure sliding mode controlled induction motor drive," in Proc. 25th Annual IEEE Power Electronics Specialists Conf., Taipei, Taiwan, 20-25 June, pp. 243-249, 1994.

[8] K.-K. Shyu, C.-K. Lai, Y.-W. Tsai, and D.-I. Yang, "A newly robust controller design for the position control of permanent-magnet synchronous motor," IEEE Trans. Industrial Electronics, vol. 49, no. 3, pp. 558-565, 2002.

[9] F.-J. Lin, D.-H. Wang, and P.-K. Huang, "FPGA-based fuzzy sliding-mode control for a linear induction motor drive," IEE Proc. Electric Power Applications, vol. 152, no. 5, pp. 1137-1149, 2005.

[10] Y. Tian and Q. Guo, "Study on robustness-tracking control for linear servo system," in 4th International Power Electronics and Motion Control Conf., Xi'an, China, 14-16 Aug., pp. 1060-1064, 2004.

[11] S.-L. Chen, H.-L. Liu, and S. C. Ting, "Contouring control of biaxial systems based on polar coordinates," IEEE/ASME Trans. Mechatronics, vol. 7, no. 3, pp. 329-345, 2002.

[12] J.-W. Jeon, M. Caraiani, D.-H. Hwang, J.-H. Lee, D.-S. Kang, Y.-J. Kim, and S.-S. Kim, "High-precision and decomposition control of several permanent magnet linear motors for magnetic levitation," in 37th IEEE Power Electronics Specialists Conf., Jeju, Korea, 18-22 June, pp. 1-6, 2006.

[13] Y. Yildiz and A. Sabanovic, "Neuro sliding mode control of timing belt servo-system," in 8th IEEE International Workshop on Advanced Motion Control, Kawasaki International Center, Japan, 25-28 March, pp. 159-163, 2004.

[14] J. O. Jang, "Deadzone compensation of an XY-positioning table using fuzzy logic," IEEE Trans. Industrial Electronics, vol. 52, no. 6, pp. 1696-1701, 2005.

[15] J. H. Kim, J. H. Park, S. W. Lee, and E. K. P. Cheng, "A two layered fuzzy logic controller for systems with deadzones," IEEE Trans. Industrial Electronics, vol. 41, no. 2, pp. 155-162, 1994.

[16] F. L. Lewis, W. K. Tim, L. Z. Wang, and Z. X. Li, "Deadzone compensation in motion control systems using adaptive fuzzy logic control," IEEE Trans. Control Systems Technology, vol. 7, no. 6, pp. 731-742, 1999.

[17] S. Y. Oh and D. J. Park, "Design of new adaptive fuzzy logic controller for nonlinear plants with unknown or time-varying dead zones," IEEE Trans. Fuzzy Systems, vol. 6, no. 4, pp. 481-492, 1998.

[18] G. Ellis, Control System Design Guide, Academic Press, California, 2000.